

# **Characterizing the Soil Microbiome of Invasive Halophytes in Disturbed and Non-Disturbed Sites**

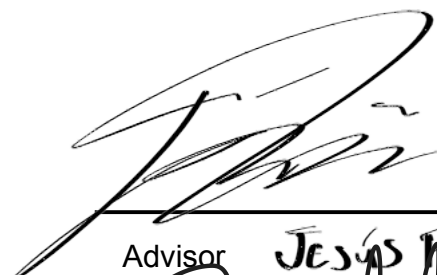

Presented to

**The Department of Organismal Biology and Ecology  
Colorado College**

By Bachelor of Arts, December 2025

Riley Johnn Kadis

Edited by Dr. Jesús Peña and Dr. Rachel Jabaily

  
\_\_\_\_\_  
Advisor **JESÚS F. PEÑA** 4/25/2025  
  
\_\_\_\_\_  
Second reader

## Acknowledgments:

I want to extend my gratitude to Dr. Shane Heschel and the members of the Heschel Lab for their field support. Additionally, I thank Tia Hutchens, Ali Keller, and Dr. Rachel Jabaily for their technical support. I also want to thank the Colorado College Natural Sciences Executive Committee, the CC Organismal Biology and Ecology Department, and the Hevey Family Fund for funding this work. Finally, I want to thank Dr. Jesús F. Peña for his generous guidance and support.

## Introduction

The invasion of riparian zones in the western United States by *Tamarix* (saltcedar) has transformed the ecology and composition of these systems. Originally introduced in the early 19th century for erosion control and as an ornamental (Sher and Quigley, page 3), *Tamarix* has since proliferated at the expense of native riparian vegetation like *Populus fremontii* (cottonwood) and *Salix* species (willow) (Glenn et al., 2005). This shift is tied to anthropogenic modifications of hydrology, including dam construction, river regulation, and reductions in overbank flooding. These changes have rendered floodplains more arid and saline. Studies of other invasive plant species have yielded the Degraded Mutualism Hypothesis (Řezáčová et al., 2020) which predicts that invasive plants may suppress or fail to support native mutualists, particularly arbuscular mycorrhizal fungi, to the detriment of co-occurring native species. Conversely, the Enhanced Mutualist Hypothesis predicts that some invasive plants gain disproportionate benefits from existing microbial symbionts. In either case, changes to microbial networks can shift competitive balances belowground, but this framework has not yet been applied to *Tamarix*'s invasion of North America.

The Fountain Creek Watershed is one environment with dramatic anthropogenic changes in water flow. Centered around Colorado Springs and extending to Pueblo, the watershed is a 927 square-mile area that drains to the Arkansas River in Pueblo, Colorado (Fountain Creek Watershed District, 2025). Our study site lies within the Fountain Creek floodplain near the Fountain Creek Regional Park, 15 miles south of Colorado Springs. This site has a dynamic disturbance history, with 85% of Colorado Springs' water being pumped across the Continental Divide and discharged into Fountain Creek after use (Fountain Creek Watershed District, 2025). This contributed to regular damaging floods and pollution (Fountain Creek Watershed District, 2009), such as in 2005 when a series of spills released 377,000 gallons of raw wastewater into Fountain Creek (Theo Stein, Denver Post. 2005). However, this flooding has been reduced by drainage and erosion mitigation projects by the Fountain Creek Watershed District since its formation in 2009 (Fountain Creek Watershed District, 2025).

As a halophyte, *Tamarix* is well adapted to tolerate drought and salt stress (Shafroth et al., 1995; Glenn et al., 2005). It exhibits traits that enhance its success in disturbed riparian

environments. These include high salt and drought tolerance, rapid seed production with flexible timing, fire resistance, and the ability to resprout after disturbance (Glenn et al., 2005). Moreover, *Tamarix* can alter the chemical properties of the soil it inhabits. Through salt extrusion and leaf abscission, it can raise soil salinity and modify nutrient availability over time, creating feedback loops that further suppress native vegetation (Shafroth et al., 1995). This behavior appears allelopathic and increases the plant's salt tolerance, but its mechanisms are understudied (Imada et al., 2012). Chemical extrusion also allows *Tamarix* to engineer its environment through the formation of “fertile islands”—localized zones beneath plant canopies where organic matter and nutrients accumulate. In coastal and desert ecosystems, *Tamarix* species have been shown to generate steep vertical and horizontal gradients in nitrogen and phosphorus availability, especially in the topsoil (Rong et al., 2016). As *Tamarix* manipulates the concentration of soil nutrients, it may be able to change the limiting nutrient of its surrounding environment (Rong et al., 2016), impacting microbial activity and nutrient cycling, with potential consequences for plant–microbe interactions. Comparatively, one study found *Populus*' effect on soil nitrogen content is variable, but possibly negative as net Nitrogen mineralization was substantially lower in cottonwood compared to conifer plots in the field (Sabau et al., 2010). However, this study looked at *Populus trichocarpa* (black cottonwood) in a coastal hemlock forest rather than *Populus fremontii* (plains cottonwood) in a high desert riparian setting (US Department of Commerce, 2021) and did not include salinity measurements. Another study found total soil Nitrogen was significantly less in a native *Populus tremuloides* (quaking aspen) forest in Saskatchewan than in managed *Medicago sativa* (alfalfa) fields (Yannikos et al., 2014) but again this is a different species in a different environment, being compared to a legume cultivated for nitrogen fixation.

Bacteria and fungi may have lower diversity under *Tamarix*'s chemical regimes, as microbial diversity tends to be lower in more saline environments (Yang et al., 2023). Additionally, increases in salinity and nitrate content have both been found to increase pH independently and pH has been found to reduce microbial diversity even more than salinity (Yang et al., 2023). However, total soil nitrogen tends to increase fungal diversity (Yang et al., 2023) and increases in salinity have been found to alter biotic activity and reduce denitrification, perhaps contributing to the accumulation of nitrate in the soil (Pan et al., 2023). Thus, while *Tamarix*'s altering of soil chemistry makes it a keystone species in Lanzhou Bay, China, where it



stabilizes sand and water, buffers wind, and supports biodiversity (Rong et al., 2016), it may influence the structure and function of soil microbial communities, particularly in arid and semi-arid systems by directly altering the soil stoichiometry created by natural wind and water patterns (Aguiar & Sala, 1999). Altering soil stoichiometry could contract the niche of microbes which rely on key metabolic pathways and cycle nutrients through the system, while expanding the niche of others. Additionally, arid ecosystems often function as two-phase mosaics with high-cover patches acting as fertility islands surrounded by low-cover vegetation that conserves water and nutrients, while supporting rich microbial networks (Aguiar & Sala, 1999). However, with *Tamarix*'s allelopathic behavior deterring low cover vegetation from establishing within its canopy, it may also prevent an independently functioning nutrient network from forming. Other halophytes such as *Halopeplis perfoliata* rely on symbiotic bacteria that empower them to tolerate harsh abiotic stressors, but few studies have examined the soil microbiome in relation to halophytes (Baeshen et al., 2023). This raises the question of whether *Tamarix* recruits beneficial microbes, further altering the microbial community and facilitating its global invasion. Despite the growing body of research on the role of microbial communities in plant establishment and success, and the estimated 80% of plants that form mycorrhizal association (Liu et al., 2020) the specific composition and ecological function of the *Tamarix* soil microbiome remains underexplored, particularly in North America. *Tamarix* in Saudi Arabia have been found to have the highest bacterial species richness localized in their proximate soil crust, and fungal species richness in their rhizosphere (Baeshen et al., 2023), but there is limited research into how *Tamarix* interacts with these microbes, how that affects neighboring plants, and if this pattern holds in North America. With soil microbial communities being influenced by their plant community, but governed mostly by climatic factors (Liu et al., 2020), it seems likely Colorado soils would host distinct microbial communities.

Given this history, the present work examines the soil microbiome and nutrient dynamics associated with *Tamarix* in Fountain Creek, Colorado. Specifically, how microbial community composition, diversity, and soil chemistry vary with proximity to *Tamarix* and the presence or absence of neighboring cottonwoods. These results provide insight into the mechanisms of *Tamarix*'s interactions with the Fountain Creek community and are extrapolated to *Tamarix*'s invasion across the American southwest.

# Methods

## Sampling:

Three clusters of mature *Tamarix* were identified in Fountain Creek from undisturbed (shaded by cottonwoods) and disturbed (not shaded by cottonwoods) plots. In early June, 0.5 gallons of the top 6 inches of soil (O and A horizons) were taken along a distance gradient from each individual *Tamarix* (0m, 0.5m, 1m, 2m) and stored in Ziploc bags. Soil samples were transported in a cooler and stored long term in a refrigerator at 37°F.

## Soil Chemistry:

Nitrate content was measured in parts per million (ppm) using Spectrum Technologies LAQUA nitrate meter, with a soil slurry composed of 40mL of deionized water, 20g of soil, and 5 drops of ammonium acetate, yielding a final soil: water ratio of 1:2. The slurry was stirred for one minute and left to settle for 5 minutes before testing.

Salinity was measured in millimhos/cm from a room temperature slurry of 1:2 soil: deionized water using a Kelway Soluble Salts Detector. Because this device measures conductivity, it is not specific to NaCl and records based on all dissolved Cl<sup>-</sup> and partner ions.

ANOVAs were used to assess the relationship between status, location, salinity, and nitrate concentration. Salinity and Nitrate concentration were visualized with bar plots and interaction plots.

## Dilution and Culture:

For each sample, soil was suspended in 300mL of distilled water, and the resulting stock solution was serially diluted four times, each at a 1:10 ratio, to produce 10<sup>-1</sup> to 10<sup>-4</sup> dilutions.

Stock Solution	D1: 0.02756mg/μL	D3: 0.0471mg/ μL	D4: 0.02873mg/μ L	UD24: 0.02853mg/μL	UD26: 0.02793mg/μL	UD30: 0.02666mg/μL
Dilution 1	2.756μg/μL	4.71μg/μL	2.873μg/μL	2.853μg/μL	2.793μg/μL	2.666μg/μL
Dilution 2	0.2756μg/μL	0.471μg/μL	0.2873μg/μL	0.2853μg/μL	0.2793μg/μL	0.2666μg/μL
Dilution 3	0.02756μg/μL	0.0471μg/ L	0.02873μg/μL	0.02853μg/μL	0.02793μg/μL	0.02666μg/μL
Dilution 4	0.002756μg/μL	0.00471μg/ μL	0.002873μg/μ L	0.002853μg/μL	0.002793μg/μL	0.002666μg/μL

**Table 1:** Micrograms of soil per microliter of water. These values were calculated based on the dilution factors and original mass of soil added to the corresponding stock solution.

200  $\mu$ L of each dilution was then ejected and spread across the surface of one Luria-Bertani (LB, nutrient rich medium for bacterial culture) and one Rose Bengal Chloramphenicol Malt Extract agar (RBC, antibiotic and fungistatic) petri dish. Plates were left at room temperature for 24 hours before being wrapped in parafilm and refrigerated.

### Microscopy:

Visually different bacterial colonies on LB plates from each soil sample were mounted on slides with a sterile toothpick, resulting in one slide per soil sample. A Gram stain was performed and slides were then covered with translucent packing tape. Slides were visualized with oil immersion light microscopy under a 100x objective, with photos taken of unique regions and morphotypes on each slide. Qualitative observations were made of each slide for comparison between soil sample groups.

### DNA Extraction and Sequencing:

DNA was extracted from homogenized soil samples using the Qiagen Power Soil Pro kit per the manufacturer's instructions. A 2% agarose gel was used to assess quality. DNA concentration and purity was further assessed with a nanodrop. After passing quality control the extracted DNA was pooled by condition, combining the 0m, 0.5m, and 1m samples into a single 'inside the canopy' group for each site, yielding one DNA sample from inside, and one from outside the canopy of each *Tamarix*. The pooled DNA was sent to CD Genomics for meta-amplicon sequencing of 16S rRNA (bacteria) and ITS (fungi) regions on the Illumina platform.

### Bioinformatics and Statistics:

A rarefaction curve produced by CD Genomics was used to estimate the capture of our sequencing, and the likelihood that there are taxa present that are not represented in our dataset. Fungal ITS barcode sequences were identified using BLASTn (Altschul et al., 1990) against the FungiDB database (Basenko et al., 2018). Sequences were queried against fungal and oomycete genomes, with an expectation value cutoff of 0.05 and a maximum of 100 target sequences per query. Default BLASTn parameters were applied, including a word size of 11, match/mismatch scores of 2/-3, and gap costs of 5/2. Low-complexity regions were filtered using DUST masking. The top hit species for each sequence were then used as queries for the NCBI Taxonomy database (Schoch et al., 2020; Sayers et al., 2019) and taxonomy for each ASV was manually assigned.

Amplicon Sequence Variants with less than 10 total occurrences across groups were removed from the dataset. The DESeq function was then used in R to compare the counts of each ASV to the total data set and determine if they are ‘enriched’ (more abundant) or ‘depleted’ (less abundant) to a statistically significant degree (Love et al., 2014). The amplicon sequences of highly enriched fungal ASV’s ( $p\text{-value} \leq 0.05$ ) were subjected to a nucleotide BLAST query through [FungiDB](#) (Basenko et al., 2018), with an e-value of 10 to determine taxonomy from the species to phylum level. These designations were used in the following analysis.

Raw metabarcoding sequences assigned taxonomic classifications using the SILVA reference database (Quast et al., 2013; Yilmaz et al., 2014; Glöckner et al., 2017). Sequences were uploaded in FASTA format to the SINA (SILVA Incremental Aligner) v1.2.12 web tool for alignment and classification (Pruesse et al., 2012). The alignment was performed using the SSU (Small Subunit) reference alignment, with terminal unaligned bases attached to the last aligned base. Taxonomic classification was conducted using the SILVA database, with a minimum sequence identity threshold of 0.95 and up to 10 nearest-neighbor reference sequences considered for classification. Sequences with identity scores below 70% were excluded from downstream analyses. The resulting taxonomy assignments were then imported into phyloseq (McMurdie and Holmes, 2013) for further analysis.

Shannon, Chao1, and Observed indices were calculated in R with the phyloseq package. Comparison of the community compositions and specific distributions of species in each sample was performed with Upset Plots with the upSetR package in R and upset function (Conway et al., 2019).

# Results

## Soil Chemistry:

**Table 1:** Summary of soil salinity and nitrate content.

Location	Status	Salinity (mmhos/cm)	Salinity Standard Error	Nitrate (ppm)	Nitrate Standard Error
Outside canopy	Disturbed	0.07	0.039	39	9.02
		0.2	0.039	67	9.02
		0.166	0.039	41	9.02
Outside canopy	Non-disturbed	0.06	0.207	41	6.77
		0.1	0.207	63	6.77
		0.7	0.207	45	6.77
Within canopy	Disturbed	0.186	0.144	91	12.66
		0.15	0.144	77	12.66
		0.6	0.144	120	12.66
Within canopy	Non-disturbed	0.07	0.103	50	53
		0.4	0.103	53	53
		0.35	0.103	56	53

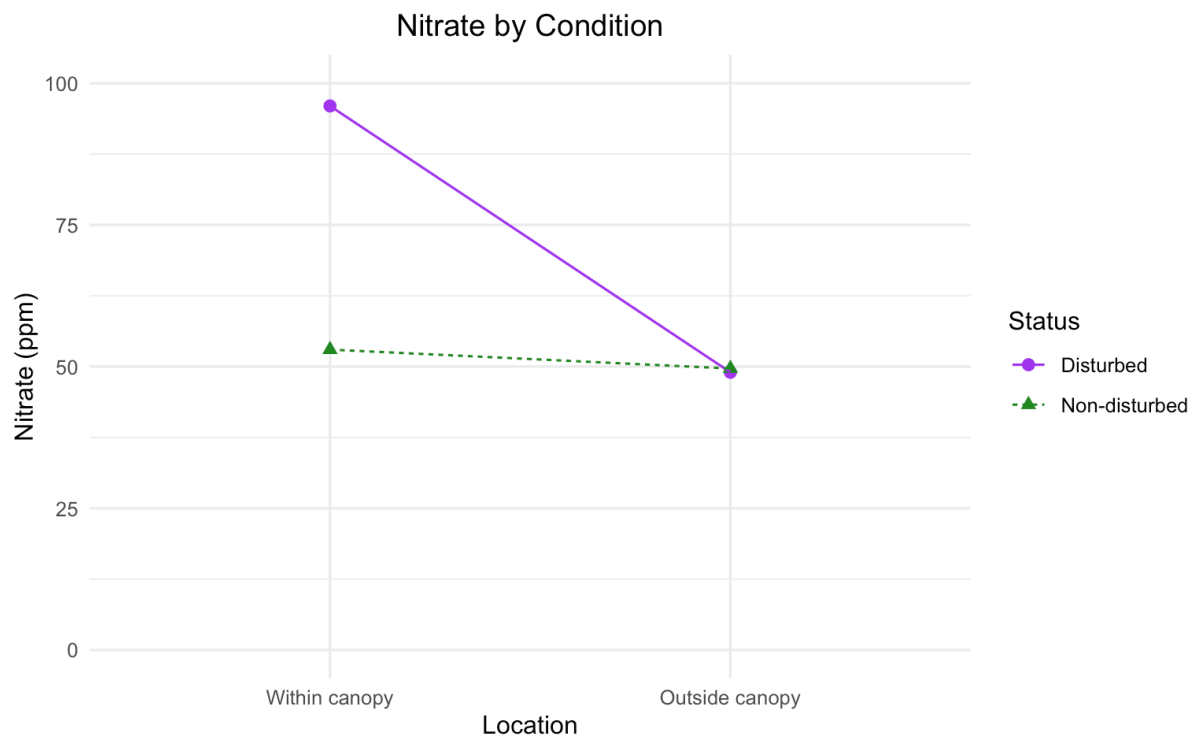


**Figure 1:** Interaction plot of average nitrate content in soil from within and outside the *Tamarix* *sp.* canopy for disturbed and non-disturbed sites.

Nitrate concentrations varied by both canopy location and disturbance status (Table 1), with a notable interaction between the two factors (Fig. 1). In disturbed sites, average nitrate levels were substantially higher within the canopy but dropped steeply outside the canopy (Fig. 1, Tables 1). In non-disturbed areas, nitrate levels remain relatively stable regardless of location, but still show a slight decrease (Fig. 1, Table 1).

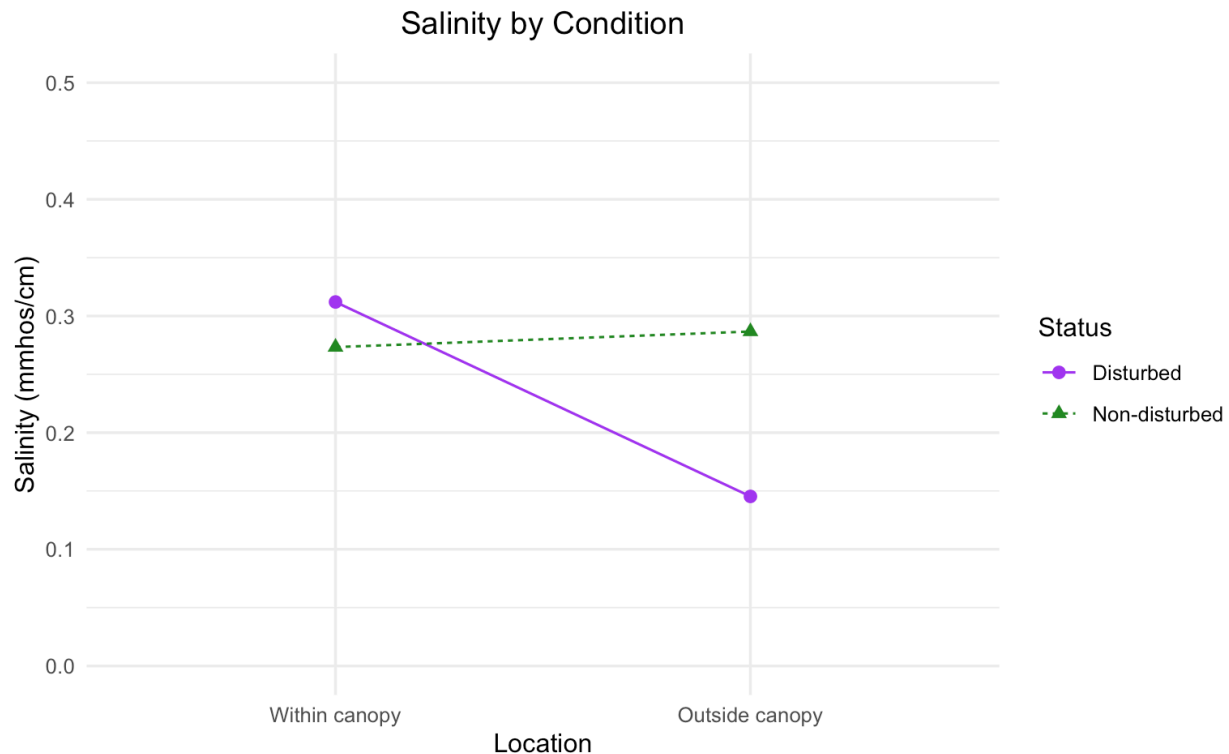


**Figure 2:** Interaction plot of average salinity if soil from within and outside the *Tamarix* canopy for disturbed and non-disturbed sites.

Like nitrates, salinity also varied by both location and status (Table 1, Fig. 2). The average salinity was higher within the canopy of disturbed areas, but decreased sharply outside the canopy (Fig. 2, Table 1); this pattern parallels what was observed for nitrates (Fig. 1). In non-disturbed areas, salinity remains relatively constant, but in contrast to nitrates, it slightly increases outside the canopy (Fig. 1).

With both salinity and nitrate, concentrations differed more in disturbed sites, with concentrations being much higher within the *Tamarix* canopy (Fig. 1 and 2). In the non-disturbed sites, the average salinity was less than 0.5mmhos/cm under the average salinity of disturbed plots within the canopy (Fig. 2). However, the average nitrate of the undisturbed plots was only slightly above the average of disturbed plots outside the *Tamarix* Canopy (Fig. 1).

A significant relationship between salinity and disturbance status ( $F(1)=0.139$ ,  $p>0.1$ ), salinity and location ( $F(1) = 0.31$ ,  $p>0.1$ ), or status and location with respect to salinity ( $F(1) = 0.428$ ,  $p>0.1$ ) were not detected. However, significant relationships between nitrate and status ( $F(1) = 6.170$ ,  $p<0.05$ ), nitrate and location ( $F(1) = 8.723$ ,  $p<0.05$ ), and status and location with respect to nitrate ( $F(1) = 6.565$ ,  $p<0.05$ ) are supported. A subsequent analysis with one-way ANOVAs did not support a significant relationship between salinity and status ( $F(1) = 0.159$ ,  $p>0.1$ ), nitrate and status ( $F(1) = 2.65$ ,  $p>0.1$ ), salinity and location ( $F(1) = 0.362$ ,  $p>0.1$ ), or salinity and nitrate ( $F(1) = 1.256$ ,  $p>0.1$ ). However, a weak relationship between nitrate and location ( $F(1) = 4.207$ ,  $p<0.1$ ) was supported.



## Gram Stain:

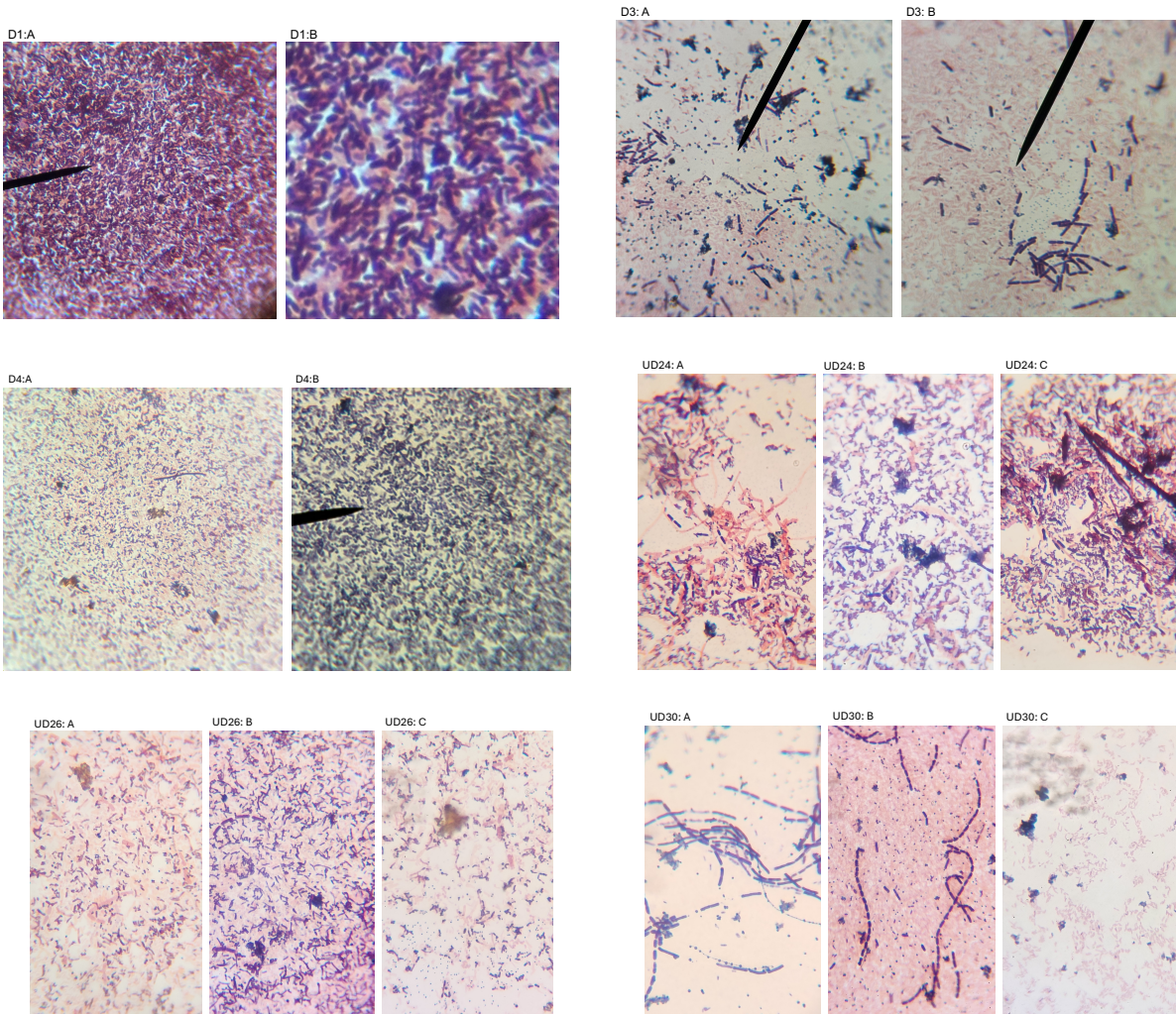


**Figure 3:** Gram stain images from each soil sample. Photos were selected to show different morphologies and reflect the broad patterns found across the slides. All images were taken under 100x oil immersion. (D=disturbed soil samples, UD=undisturbed samples)

Observationally, Gram staining revealed a higher proportion of Gram+ bacteria across disturbed samples than in undisturbed samples, and vice versa. However, slides from UD30 had larger organized aggregates of Gram+ bacteria than any other sample.



## Metabarcoding:

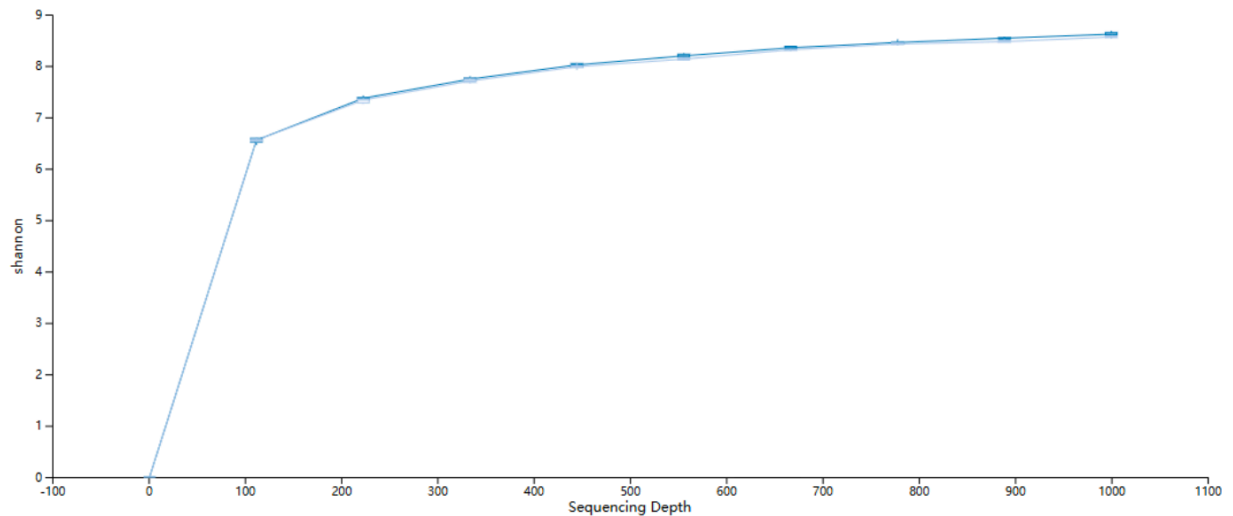


**Figure 4:** Rarefaction curve created by randomly selecting a certain amount of 16S (bacterial) sequencing data from the samples, then counting the number of the species these data represent. The darker curve represents the data from disturbed samples while the lighter represents undisturbed samples.

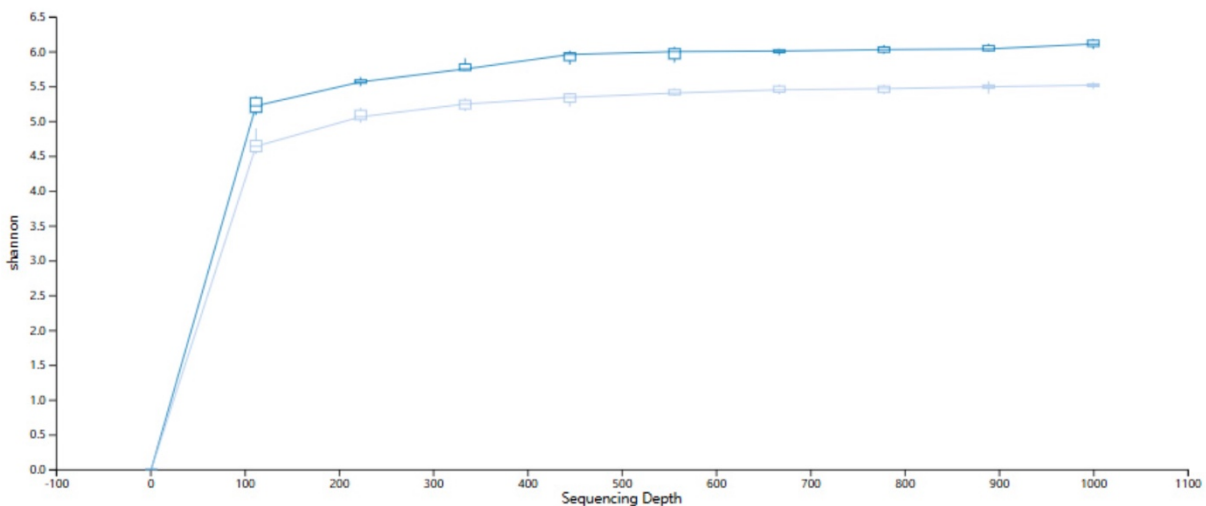


**Figure 5:** Rarefaction curve created by randomly selecting a certain amount of ITS (fungal) sequencing data from the samples, then counting the number of the species these data represent. The darker curve represents the data from disturbed samples while the lighter represents undisturbed samples.

Rarefaction curves can be used to judge the sequencing sufficiency of each sample. The steep sloped portion represents newly discovered species diversity, while the flatter portion represents already discovered species. That both rarefaction curves level off rapidly suggests that

further sequencing is likely to yield few unique new species. Thus, our sequencing efforts likely captured a very high percentage of the actual microbes present in the sample.

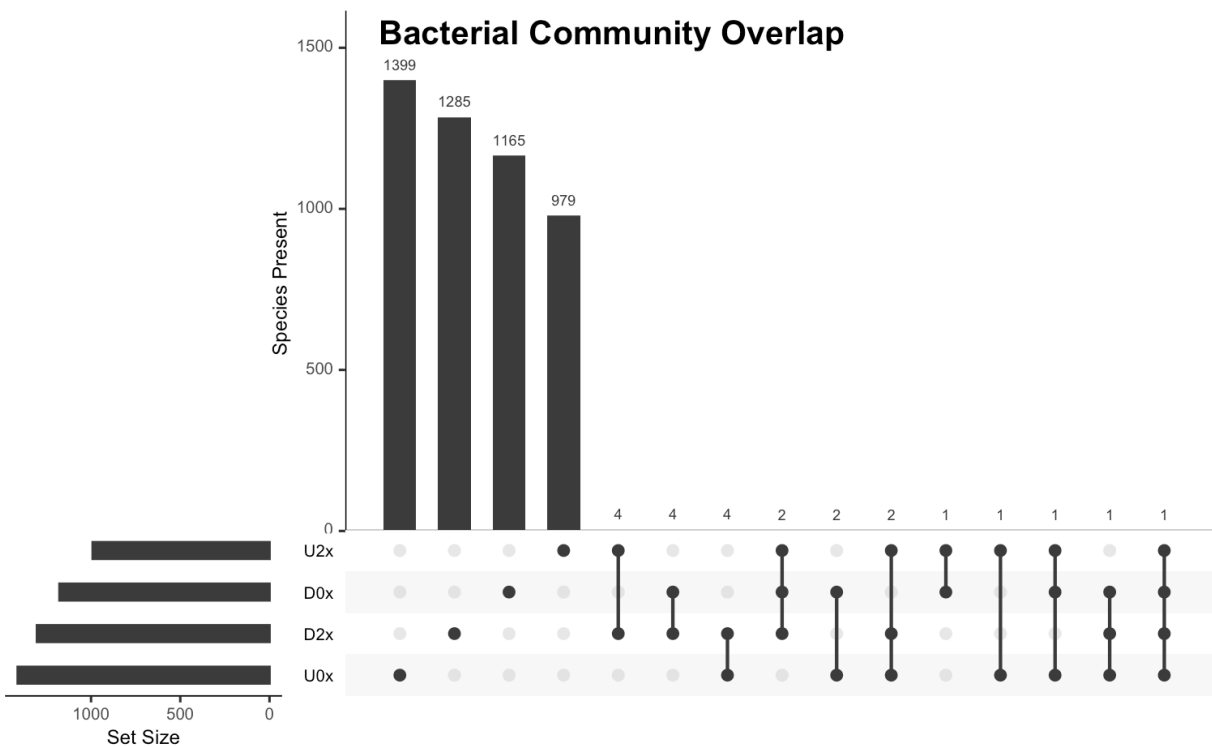


**Figure 6:** Comparison of overlapping bacterial ASVs between sites. Vertical bars represent the number of taxa unique to or shared between the sample combinations indicated by the connected black dots beneath them. Horizontal bars indicate the total number of taxa observed in each sample. Sample names refer to combinations of disturbance status (U=non-disturbed, D=disturbed) and location (0x=within canopy, 2x=outside canopy).

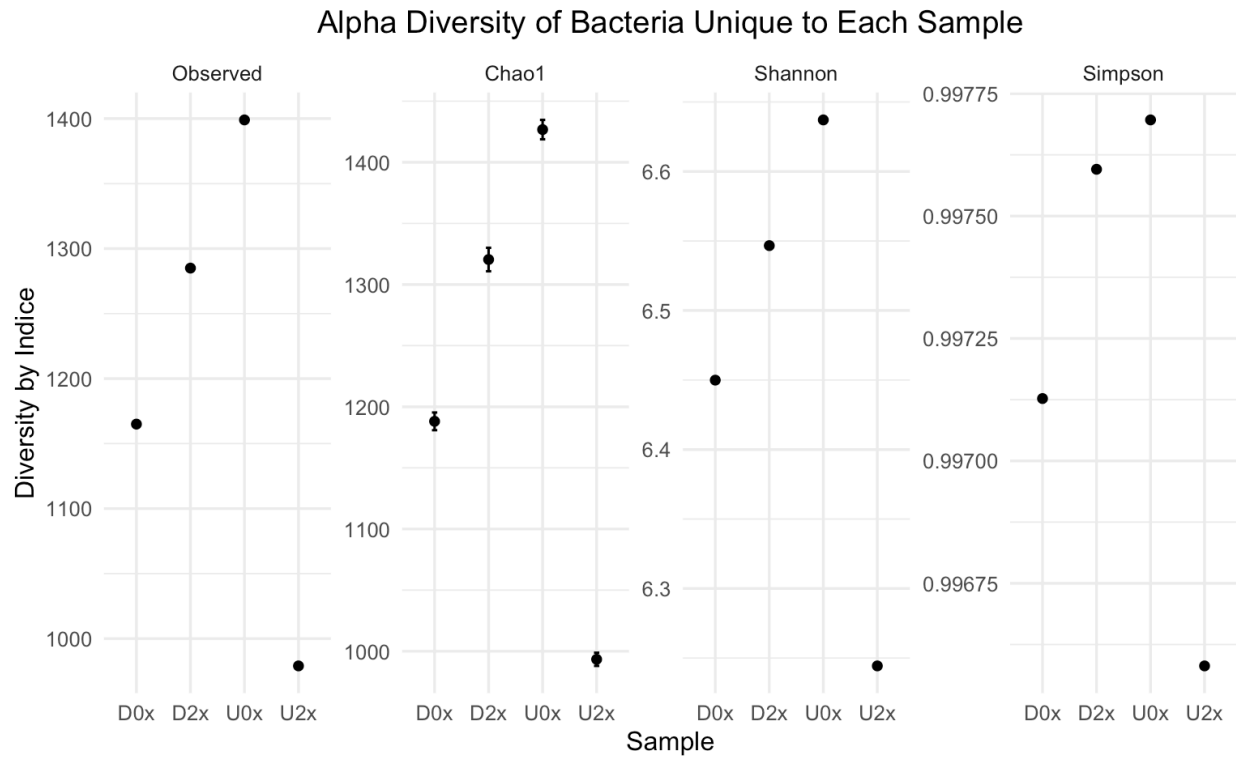


**Figure 7:** Diversity indices calculated using bacterial ASVs which were unique to one sample: the first 4 vertical bars of figure 4.

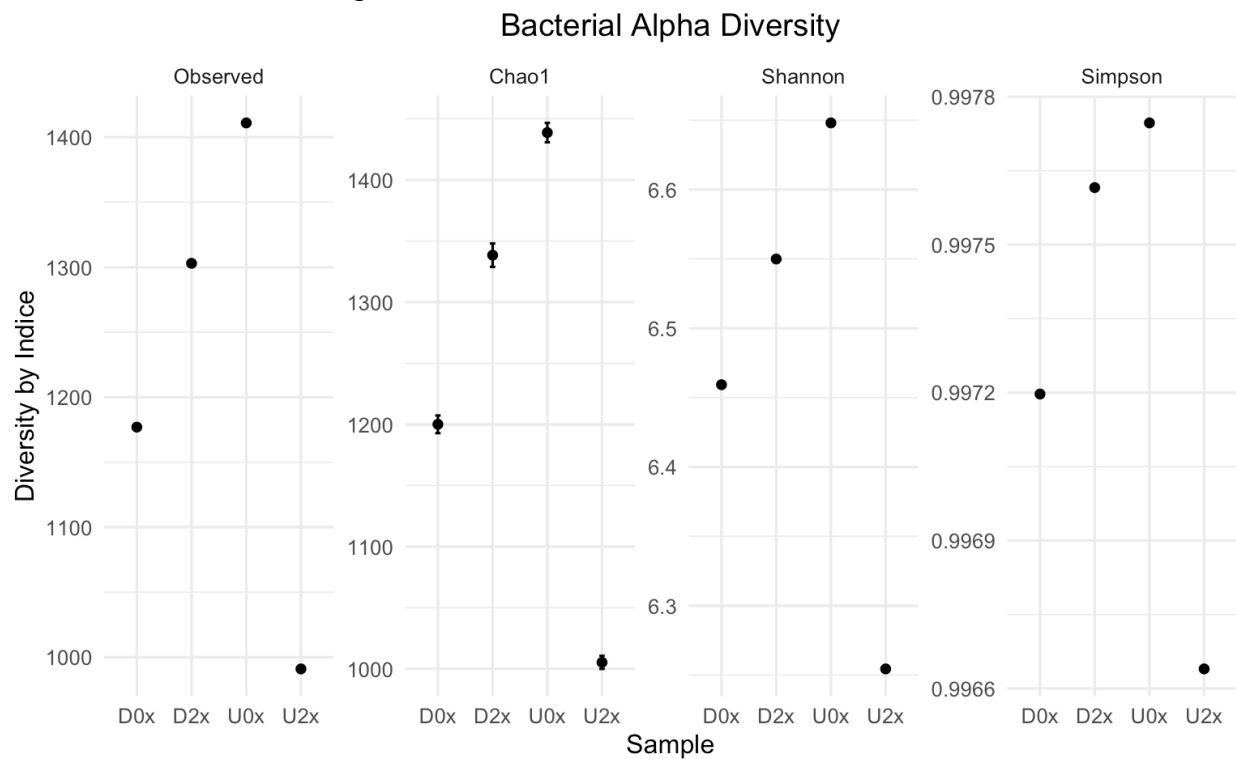


**Figure 8:** Diversity indices calculated from all identified bacterial ASVs among all samples.

Bacterial communities differed significantly among sample groups, with no more than 4 taxa being shared among any given combination of groups (Fig. 6). The values for a specific group did not differ in rank between Observed, Chao1, Shannon, and Simpson, indices. However bacterial diversity in disturbed plots outside the canopy is closer to the samples from non-disturbed site within the canopy (Fig. 7 and 8). By each metric, the most diverse plots were undisturbed plots within the canopy, and by far the least diverse plots were undisturbed outside the canopy. Disturbed plots did not differ as much in bacterial diversity. Additionally, both fell within the range of the undisturbed plots, with higher diversity outside the *Tamarix* canopy.

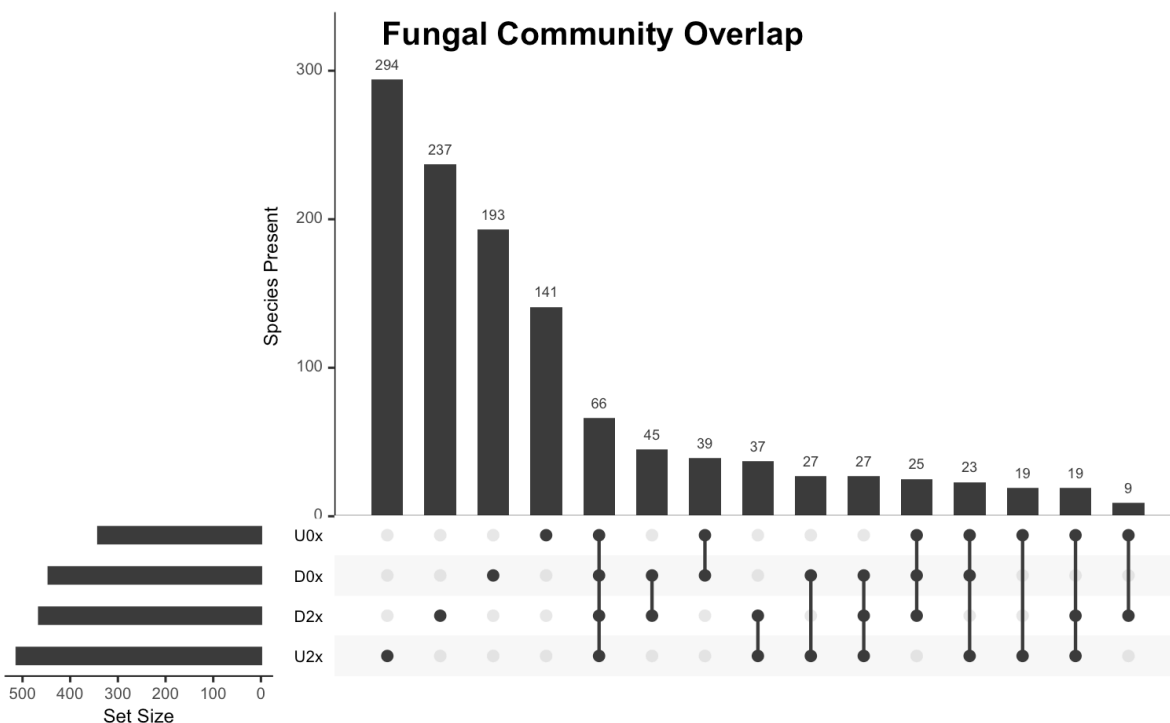


**Figure 9:** Comparison of overlapping Fungal ASVs between sites. Vertical bars represent the number of taxa unique to or shared between the sample combinations indicated by the connected black dots beneath them. Horizontal bars indicate the total number of taxa observed in each sample. Sample names refer to combinations of disturbance status (U=non-disturbed, D=disturbed) and location (0x=within canopy, 2x=outside canopy).

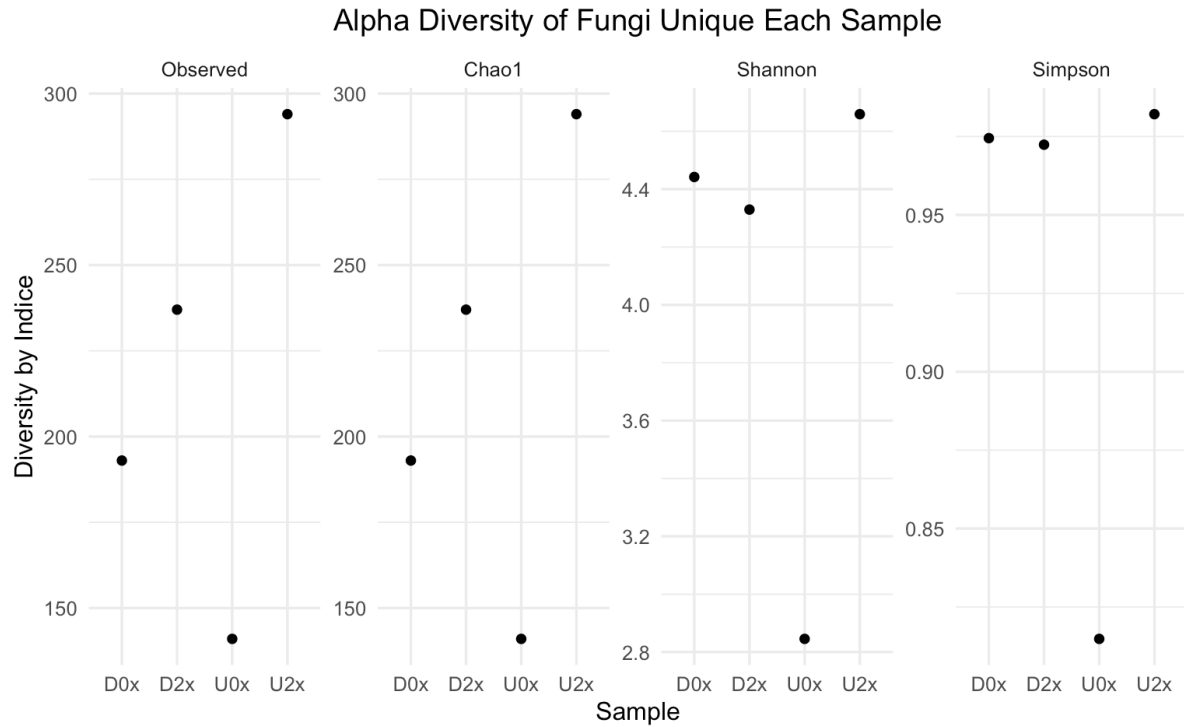


**Figure 10:** Diversity indices calculated using fungal ASVs which were unique to one sample: the first 4 vertical bars of Figure 4.

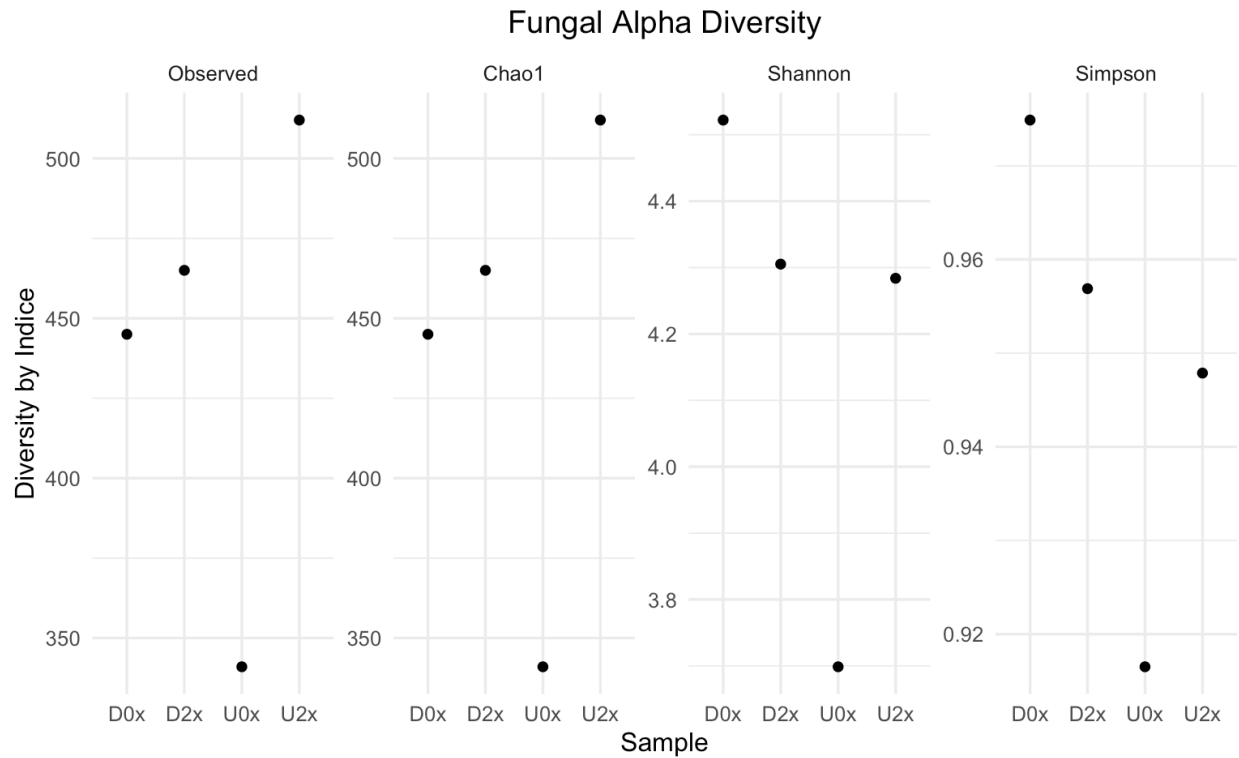


**Figure 11:** Diversity indices calculated from all identified fungi among all samples.

Fungal communities were far more similar between sample groups than bacteria (Fig. 6 and 9) but still overlapped little. There were more fungal taxa present in all samples than any other combination of samples, but most of the taxa present at any given site were only present at that site (Fig. 9).

When looking at the fungi unique to each sample, undisturbed sites still held the minimum and maximum of fungal diversity but with the lowest diversity inside the *Tamarix* canopy, and highest outside it (Fig. 10). Fungal diversity of disturbed plots also does not vary as much as undisturbed plots, but with significant differences between indices: Observed and Chao1 diversity of disturbed plots were staggered between the maximum and minimum of the undisturbed plots, but the Shannon and Simpson diversity of the disturbed plots were only slightly less than outside the canopy non-disturbed site diversity, with Simpson diversity being higher than Shannon (Fig. 10).

When looking at all identified fungi, ranking varied by index. Undisturbed samples within the *Tamarix* canopy had the lowest diversity by all metrics, while undisturbed samples outside the canopy had the highest according to the Observed and Chao1 indices, and intermediate values less than those of the disturbed plots according to the Shannon and Simpson indices (Fig. 11). Disturbed plots had intermediate values slightly closer to the maximum according to the Observed and Chao1 indices, with samples from outside the canopy having slightly higher diversity than inside. Shannon and Simpson indices both recorded disturbed plots inside the canopy as having the most diversity and disturbed plots outside the canopy the second most, with disturbed outside being closer to undisturbed outside than disturbed inside, but closer to the maximum in Shannon than in Simpson (Fig. 11).

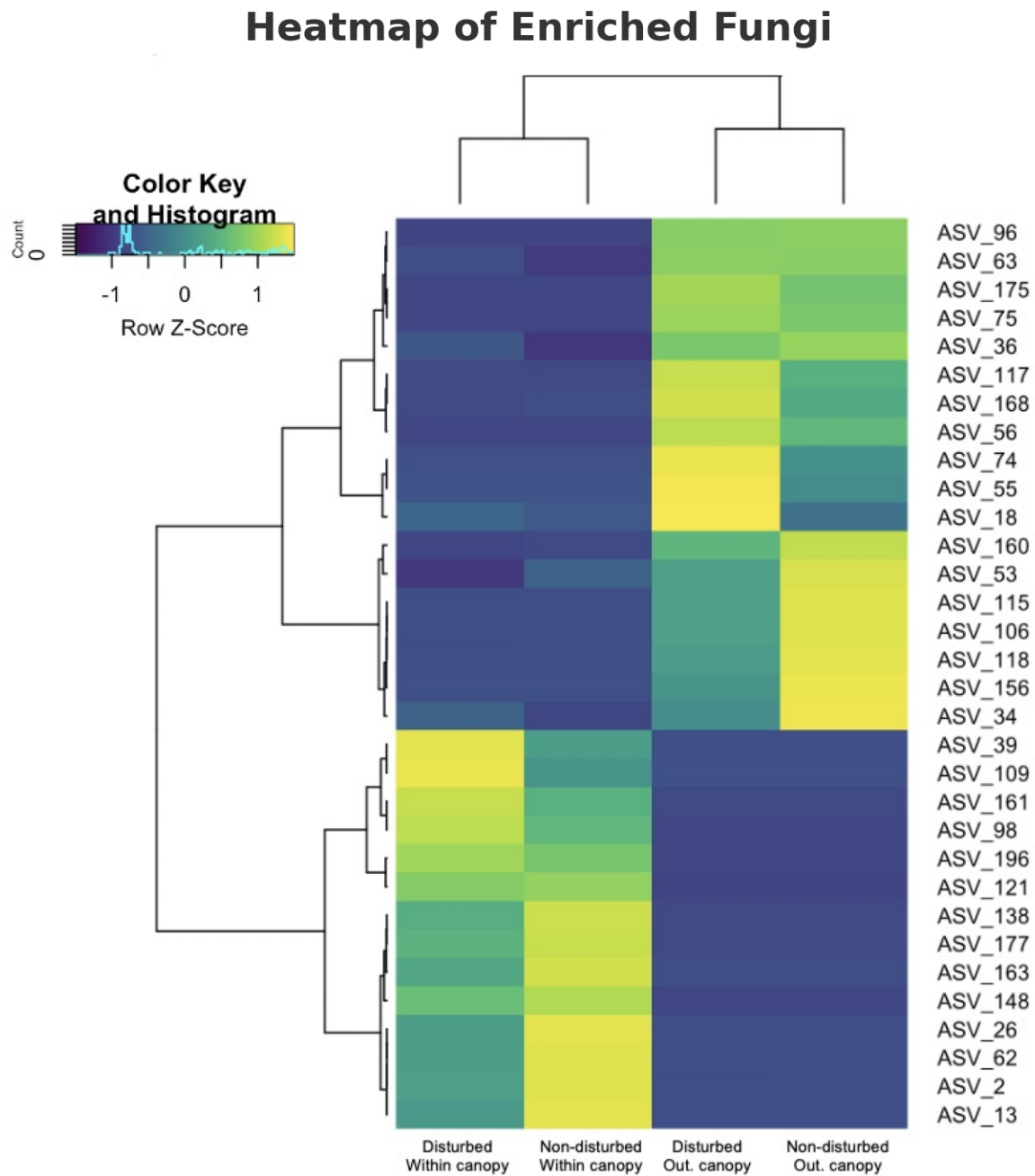


**Figure 10 (12):** heatmap indicating the abundance of the most enriched fungal ASVs across sample groups.

**Table 2:** Key to enriched fungal ASVs. The species name, nutritional mode, and primary location each correspond to the ASV ID on the left, and that row in figure 10.

ASV	BLAST Identification	Ecology	Location
ASV_96	<i>Ascomycota Sclerotinia sclerotiorum</i> 1980 UF-70	Generalist plant pathogen (Derbyshire et al., 2017)	Outside Canopy
ASV_63	<i>Parastagonospora nodorum</i> SN15	Necrotroph (Kariyawasam et al., 2023)	Outside Canopy
ASV_175	<i>Aspergillus aculeatus</i> ATCC 16872	Saprotroph (Grigoriev et al., 2012)	Outside Canopy
ASV_75	<i>Aspergillus lentulus</i> strain IFM 54703	Opportunistic human pathogen (Swilaiman 2013)	Outside Canopy
ASV_36	<i>Curvularia clavata</i> yc1106	Generalist plant pathogen (Cao et al., 2023)	Outside Canopy
ASV_117	<i>Neurospora discreta</i> FGSC 8579	Saprotroph (Grigoriev et al., 2012)	Outside Canopy
ASV_168	<i>Neurospora discreta</i> FGSC 8579	Saprotroph (Grigoriev et al., 2012)	Outside Canopy
ASV_56	<i>Curvularia clavata</i> yc1106	Generalist plant pathogen (Cao et al., 2023)	Outside Canopy
ASV_74	<i>Curvularia clavata</i> yc1106	Generalist plant pathogen (Cao et al., 2023)	Outside Canopy
ASV_55	<i>Fusarium verticillioides</i> 7600	Opportunistic human pathogen (Douglas et al., 2016) plant endophyte (Xia et al., 2020) and opportunistic pathogen (Masotti et al., 2023)	Outside Canopy
ASV_18	<i>Parastagonospora nodorum</i> SN15	Necrotroph (Kariyawasam et al., 2023)	Outside Canopy
ASV_160	<i>Colletotrichum graminicola</i> M1.001	Endophyte and plant pathogen (Sukno et al., 2008)	Outside Canopy
ASV_53	<i>Aspergillus campestris</i> IBT 28561	Unknown, probably plant or animal pathogen and saprotroph (Grigoriev et al., 2012)	Outside Canopy
ASV_115	<i>Fusarium verticillioides</i> 7600	Opportunistic human pathogen (Douglas et al., 2016) plant endophyte (Xia et al., 2020) and opportunistic pathogen (Masotti et al., 2023)	Outside Canopy
ASV_106	<i>Aspergillus steynii</i> IBT 23096	Unknown, possibly saprotroph (Grigoriev et al., 2012)	Outside Canopy
ASV_118	<i>Aspergillus aculeatus</i> ATCC 16872	Saprotroph (Grigoriev et al., 2012)	Outside Canopy
ASV_156	<i>Sclerotinia sclerotiorum</i> 1980 UF-70	Generalist plant pathogen (Derbyshire et al., 2017)	Outside Canopy
ASV_34	<i>Sclerotinia sclerotiorum</i> 1980 UF-70	Generalist plant pathogen (Derbyshire et al., 2017)	Outside Canopy



ASV_39	<i>Pseudogymnoascus destructans</i> 20631-21	Bat Pathogen (Urbina et al., 2021)	Within Canopy
ASV_109	<i>Aspergillus steynii</i> IBT 23096	Unknown, possibly saprotroph (Grigoriev et al., 2012)	Within Canopy
ASV_161	<i>Colletotrichum graminicola</i> M1.001	Endophyte and plant pathogen (Sukno et al., 2008)	Within Canopy
ASV_98	<i>Fusarium verticillioides</i> 7600	Opportunistic human pathogen (Douglas et al., 2016) plant endophyte (Xia et al., 2020) and opportunistic pathogen (Masotti et al., 2023)	Within Canopy
ASV_196	<i>Neurospora discreta</i> FGSC 8579	Saprotroph (Grigoriev et al., 2012)	Within Canopy
ASV_121	<i>Fusarium verticillioides</i> 7600	Opportunistic human pathogen (Douglas et al., 2016) plant endophyte (Xia et al., 2020) and opportunistic pathogen (Masotti et al., 2023)	Within Canopy
ASV_138	<i>Magnaporthiopsis poae</i> ATCC 64411	Poa pathogen (Grigoriev et al., 2012)	Within Canopy
ASV_177	<i>Curvularia clavata</i> yc1106	Generalist plant pathogen (Cao et al., 2023)	Within Canopy
ASV_163	<i>Fusarium verticillioides</i> 7600	Opportunistic human pathogen (Douglas et al., 2016) plant endophyte (Xia et al., 2020) and opportunistic pathogen (Masotti et al., 2023)	Within Canopy
ASV_148	<i>Aspergillus steynii</i> IBT 23096	Unknown, possibly saprotroph (Grigoriev et al., 2012)	Within Canopy
ASV_26	<i>Fusarium verticillioides</i> 7600	Opportunistic human pathogen (Douglas et al., 2016) plant endophyte (Xia et al., 2020) and opportunistic pathogen (Masotti et al., 2023)	Within Canopy
ASV_62	<i>Sclerotinia sclerotiorum</i> 1980 UF-70	Generalist plant pathogen (Derbyshire et al., 2017)	Within Canopy
ASV_13	<i>Histoplasma capsulatum</i> WU24	Saprotroph, mammal pathogen (Mobo et al., 2010)	Within Canopy
ASV_2	<i>Histoplasma capsulatum</i> WU24	Saprotroph, mammal pathogen (Mobo et al., 2010)	Within Canopy

# Discussion

## Soil Chemistry:

Our results diverge from prior studies in the undisturbed plots. The homogenization of soil chemistry and even reversing of the salinity gradient where cottonwoods are present is novel. The history of *Tamarix* invasion aligns with the expectation that if cottonwoods manipulate soil chemistry, they will reduce salt and nitrate concentrations. However, while cottonwoods tolerance of soil chemistry conditions is somewhat studied, the effects of cottonwoods on their proximate soil remain understudied and largely unknown. Our results call for further study of cottonwood dominated soils, particularly in riparian saline environments, and of the mechanisms by which cottonwoods may manipulate their environment.

These findings do partially reflect prior studies such as Rong et al. (2016), in revealing a chemical gradient which decreases concentration with increased distance from *Tamarix* canopy centers. Additionally, their finding that this gradient was strongest in the topsoil suggests our sampling would capture this pattern. Rong et al. (2016) did find that in coastal wetlands horizontal variations may not be important at the community level, however the history of altered flow along Fountain Creek and reduced frequency of flooding events which would flush salt through the system or fully saturate topsoil allows accumulation of salt and may amplify this effect relative to their study site.

## Distribution of Microbial Diversity Across Conditions:

When cottonwoods are not present and soil chemistry is variable, fungi are more diverse in soils with more concentrated soil chemistry, and bacteria are less diverse. With a lack of study into the environmental conditions and physiological mechanisms that mediate *Tamarix* salt extrusion, future research could investigate whether salt extrusion is a plastic behavior influenced by soil nitrogen content, which allows *Tamarix* to hold nitrogen in proximate soil.

When cottonwoods are present and soil nitrogen is consistent, fungal diversity is higher outside the *Tamarix* canopy, and bacterial diversity is far lower. This suggests that *Tamarix* does not directly support proximate fungi, whether that be through root exudates, habitat creation, or direct mycorrhizal association. This would be consistent with the Degraded Mutualism

Hypothesis and oppose the Enhanced Mutualist Hypothesis. This also reflects the results of Titus et al. (2002) which found that *Tamarix* of the Mojave Desert were non-mycorrhizal.

At the surface level, these findings oppose each other—our data suggest that *Tamarix* associates more with bacteria than fungi but also engineers its surrounding soil chemistry to favor fungi at the expense of bacteria. With the lack of enriched mycorrhizal fungi in our data set, and documented trends of soil nutrients and depth in *Tamarix* soils, it appears that *Tamarix* is concentrating nutrients in its proximate topsoil while also acting according to the Degraded Mutualism Hypothesis, in turn excluding any present mycorrhizae and its plant neighbors from vital resources. With strong niche partitioning according to depth leading to higher fungal competition in shallower soil, but a higher proportion of mycorrhizae at greater depths being observed in forest soils (Mundra et al., 2021), symbiotic fungi should have but may not have been captured in our sampling of the top 6 inches of soil. This means that further research and identification of fungi deeper in *Tamarix*'s rhizosphere and tissues, as well as mapping of the Fountain Creek mycorrhizal community may be necessary to confirm this.

When comparing the distribution of diversity across conditions, we find that fungal communities are more similar in composition across conditions than bacteria, but both are very specific to each site. This demonstrates that both *Tamarix* and *Populus* are likely affecting the microbial community, whether that be through direct association or manipulation of soil chemistry. Additionally, the presence of fungal genotypes which are distributed across sites suggests that there are fungal taxa playing key roles in the Fountain Creek plant community and linking *Tamarix* and *Populus* ecologically, whether those fungi be pathogens, saprotrophs, or plant symbionts. Our enrichment analysis shows the same lack of overlap in diversity between conditions and details that the most abundant fungal genotypes are among those specific to each site, rather than those shared (Fig. 12). It also finds that the most abundant fungi are mostly saprotrophs and plant pathogens, further suggesting a nutrient hoarding behavior by *Tamarix* (Table 2). If *Tamarix* freely exchanged nutrients, symbiotic fungi would be supported and likely be more abundant in the dataset. However, without sampling deeper in the soil and sampling of foliar endophytes and mycorrhizae within the plant's tissues, this is inconclusive.

Additionally, finding that different ASVs of generally ubiquitous saprotrophic genera of fungi like *Aspergillus* (Kwong et al., 2013) are grouped by condition suggests that different metabolic toolkits are needed to decompose plant tissues at those sites, and that *Tamarix*,

*Populus*, and varied soil chemistry may be altering nutrient cycling and flow through the Fountain Creek community. The relative lack of diversity in enriched endophyte taxa is also surprising, as they are found in the photosynthetic tissues of all major plant lineages (Apigo, A., & Oono, R., 2022) and so should be abundant in the litter layer surrounding a deciduous shrub. This could be explained by a low association between *Tamarix* and symbiotic fungi, but further research and tissue metagenomics are necessary to validate this. The presence of several animal pathogens is also curious, particularly *Pseudogymnoascus destructans*, which is found in soils, spread by bat feces (Meteyer, 2018), and has a maximum growing temperature of 20°C (Campbell et al., 2020). *P. destructans* is the causative agent of white nose syndrome in bats, the leading cause of bat multiple mortality events (cases in which  $\geq 10$  dead bats were counted or estimated at a specific location within a year or less) in the United States (Oshea et al., 2016). Without a direct documented relationship between *Pseudogymnoascus* and any plant species, or between its bat hosts and *Tamarix*, its presence is difficult to explain. However, Mexican free-tailed bats (*Tadarida brasiliensis*) have been observed feeding on *Diorhabda* (the northern Tamarix beetle) which have been released multiple times in Colorado since 1998 as a biocontrol agent of *Tamarix* (USDA, Gaffke et al., 2022). Thus, through multitrophic interactions *Tamarix* could be supporting North American bat food sources, as well as acting as vector site for the spread of White Nose Syndrome. This is corroborated by the presence of *Histoplasma capsulatum*, which can be pathogenic and spread by bat feces (University of Adelaide Australia, 2022)

It is important to note that many fungi, including *H. capsulatum* (University of Adelaide Australia, 2022) exhibit dimorphic lifecycles, in which they switch morphologies and sometimes nutritional mode, based on environmental conditions and life stage (Souza and Tabord, 2021). Therefore, identification of fungi solely by culture-based methods may miss associations and life histories that molecular identification would catch, biasing a surface level review of fungal taxa within a large sample. While an investigation of the relative diversity of fungi exhibiting each nutritional mode, and the fulfillment of available each niche would be a valuable contribution to this study, it is unrealistic at this time because of these identification challenges and the lack of a comprehensive database which includes taxonomic designations, identifying genetic sequences, and possible nutritional modes for each morphology of each fungus included.

## Conclusion

This study's application of 16S RNA and ITS Ribosomal RNA metabarcoding, soil nitrogen and salinity testing, culture, and microscopy to the proximate soil of *Tamarix* in Fountain Creek, Colorado found strong differences in soil chemistry, microbial diversity, and soil microbial composition. These differences appear to be influenced by proximity to both *Tamarix* and *Populus fremontii*, possibly through direct manipulation by these plants as well as intermediate mechanisms such as altering soil abiotic conditions. We also identify a number of future research directions necessary to fully understand the effects of *Tamarix* and *Populus* on their surroundings. These range from evidence of a possible multitrophic influence of *Tamarix* on bat fitness, to a mechanism by which *Tamarix* may hoard resources in its proximate soil. Similar studies applying metagenomics and soil chemical analysis to the tissues of *Tamarix* and *Populus* as well as the soil microbiome of *Populus* are necessary to provide a complete picture of the biotic and abiotic gradients between the two plants and elucidate their effects on Fountain Creek soil and plant communities. New information infrastructure is identified as a massive boon to future fungal ecology studies. The mapping of mycorrhizal networks through GIS and multi-locus microsatellite DNA analysis as done by Beiler et al. (2009), or the use of stable or radioactive isotope labelling as described by Watts and Williams (2022), would detail the relationships of both *Tamarix* and *Populus* with their neighbors, and allow a more comprehensive understanding of nutrient flow through the Fountain Creek system.

## Bibliography:

1. Sher and Quigley. (2013). *Tamarix: A Case Study of Ecological Change in the American West*. Oxford University Press.
2. Edward P. Glenn, century, A. the past, Cleverly, J., Devitt, D., Ellis, L., Glenn, E., ... Frasier, G. (2005). Comparative ecophysiology of *Tamarix ramosissima* and native trees in western U.S. riparian zones. Retrieved from <https://www.sciencedirect.com/science/article/pii/S0140196304002101>
3. Shafroth, P. B., Friedman, J. M., & Ischinger, L. S. (1995). EFFECTS OF SALINITY ON ESTABLISHMENT OF *POPULUS FREMONTII* (COTTONWOOD) AND *TAMARIX RAMOSISSIMA* (SALT CEDAR) IN SOUTHWESTERN UNITED STATES. *The Great Basin Naturalist*, 55(1), 58–65. <http://www.jstor.org/stable/41712864>
4. Titus, Jonathan H.; Titus, Priscilla J.; Nowak, Robert S.; and Smith, Stanley D. (2002) "Arbuscular mycorrhizae of Mojave Desert plants," *Western North American Naturalist*: Vol. 62: No. 3, Article 8. Available at: <https://scholarsarchive.byu.edu/wnan/vol62/iss3/8>
5. Aguiar, M.n, & Sala, O. E. (1999). Patch structure, dynamics and implications for the functioning of arid ecosystems. *Trends in ecology & evolution*, 14(7), 273–277. [https://doi.org/10.1016/s0169-5347\(99\)01612-2](https://doi.org/10.1016/s0169-5347(99)01612-2)
6. Rong, Q., Liu, J., Cai, Y. *et al.* "Fertile island" effects of *Tamarix chinensis* Lour. on soil N and P stoichiometry in the coastal wetland of Laizhou Bay, China. *J Soils Sediments* **16**, 864–877 (2016). <https://doi.org/10.1007/s11368-015-1296-y>
7. Baeshen, N. N., Baz, L., Shami, A. Y., Ashy, R. A., Jalal, R. S., Abulfaraj, A. A., Refai, M., Majeed, M. A., Abuzahrah, S. S., Abdelkader, H., Baeshen, N. A., & Baeshen, M. N. (2023). Composition, Abundance, and Diversity of the Soil Microbiome Associated with the Halophytic Plants *Tamarix aphylla* and *Halopeplis perfoliata* on Jeddah Seacoast, Saudi Arabia. *Plants (Basel, Switzerland)*, 12(11), 2176. <https://doi.org/10.3390/plants12112176>
8. Liu, L., Zhu, K., Wurzbürger, N., & Zhang, J. (2020). Relationships between plant diversity and soil microbial diversity vary across taxonomic groups and spatial scales. *Ecosphere*, 11(1). doi:10.1002/ecs2.2999
9. Řezáčová, V., Řezáč, M., Gryndlerová, H. *et al.* Arbuscular mycorrhizal fungi favor invasive *Echinops sphaerocephalus* when grown in competition with native *Inula conyzae*. *Sci Rep* **10**, 20287 (2020). <https://doi.org/10.1038/s41598-020-77030-0>
10. J. Sabau, Côté, L., Maguire, D. A., ... Kleinbaum, D. G. (2010). The impact of black cottonwood on soil fertility in coastal western hemlock forest. Retrieved from <https://www.sciencedirect.com/science/article/pii/S0378112710004135>
11. Stevens, M.T., Gusse, A.C. & Lindroth, R.L. Root Chemistry in *Populus tremuloides*: Effects of Soil Nutrients, Defoliation, and Genotype. *J Chem Ecol* **40**, 31–38 (2014). <https://doi.org/10.1007/s10886-013-0371-3>
12. Nils Yannikos, Peter Leinweber, Bobbi L. Helgason, Christel Baum, Fran L. Walley, Ken C.J. Van Rees. Impact of *Populus* trees on the composition of organic matter and the soil

- microbial community in Orthic Gray Luvisols in Saskatchewan (Canada). *Soil Biology and Biochemistry*, Volume 70 (2014). <https://doi.org/10.1016/j.soilbio.2013.11.025>
13. Kwon-Chung, K. J., & Sugui, J. A. (2013). *Aspergillus fumigatus*--what makes the species a ubiquitous human fungal pathogen?. *PLoS pathogens*, 9(12), e1003743. <https://doi.org/10.1371/journal.ppat.1003743>
  14. Apigo, A., & Oono, R. (2022). Plant abundance, but not plant evolutionary history, shapes patterns of host specificity in foliar fungal endophytes. *Ecosphere*, 13(1). doi:10.1002/ecs2.3879
  15. Carol U. Meteyer. (2018). White-Nose Syndrome: Cutaneous Invasive Ascomycosis in Hibernating Bats. Retrieved from <https://www.sciencedirect.com/science/article/pii/B9780323552288000722>
  16. Lewis J. Campbell, Daniel P. Walsh, David S. Bleher, Jeffrey M. Lorch; LONG-TERM SURVIVAL OF *PSEUDOGYMNOASCUS DESTRUCTANS* AT ELEVATED TEMPERATURES. *J Wildl Dis* 1 April 2020; 56 (2): 278–287. doi: <https://doi.org/10.7589/2019-04-106>
  17. Alexander M. Gaffke, Tom L. Dudley, Daniel W. Bean, Gail M. Drus, Matthew J. Johnson, Allen E. Knutson, David K. Weaver, Sharlene E. Sing, Bruce K. Orr, David C. Thompson. *Tamarix Biological Control in North America*, Chapter 28. USDA (2022). Retrieved from [https://www.fs.usda.gov/rm/pubs\\_journals/2022/rmrs\\_2022\\_gaffke\\_a001.pdf#:~:text=Di%20orhabda%20beetles%20on%20plants%20outside%20of%20the%20genus%20Tamarix.%20As%20mentioned&text=bats%20\(Tadarida%20brasiliensis\)%20have%20been%20observed%20capturing%20adult%20beetles](https://www.fs.usda.gov/rm/pubs_journals/2022/rmrs_2022_gaffke_a001.pdf#:~:text=Di%20orhabda%20beetles%20on%20plants%20outside%20of%20the%20genus%20Tamarix.%20As%20mentioned&text=bats%20(Tadarida%20brasiliensis)%20have%20been%20observed%20capturing%20adult%20beetles)
  18. O'Shea, T. J., Cryan, P. M., Hayman, D. T. S., Plowright, R. K., & Streicker, D. G. (2016). Multiple mortality events in bats: a global review. *Mammal review*, 46(3), 175–190. <https://doi.org/10.1111/mam.12064>
  19. Dimorphic Fungal Pathogens. University of Adelaide Australia (2022). Retrieved from <https://www.adelaide.edu.au/mycology/fungal-descriptions-and-antifungal-susceptibility/dimorphic-fungal-pathogens#histoplasma-capsulatum>
  20. Ana CO Souza, Carlos P Tabord. *Epidemiology of Dimorphic Fungi*, Encyclopedia of Mycology, Volume 1, 2021.
  21. Beiler, K. J., Durall, D. M., Simard, S. W., Maxwell, S. A., & Kretzer, A. M. (2009). *New Phytologist*, 185(2), 543–553. doi:10.1111/j.1469-8137.2009.03069.x
  22. Watts-Williams, S.J. Track and trace: how soil labelling techniques have revealed the secrets of resource transport in the arbuscular mycorrhizal symbiosis. *Mycorrhiza* **32**, 257–267 (2022). <https://doi.org/10.1007/s00572-022-01080-7>
  23. Mark Derbyshire, Matthew Denton-Giles, Dwayne Hegedus, Shirin Seifbarghy, Jeffrey Rollins, Jan van Kan, Michael F. Seidl, Luigi Faino, Malick Mbengue, Olivier Navaud, Sylvain Raffaele, Kim Hammond-Kosack, Stephanie Heard, Richard Oliver, The Complete Genome Sequence of the Phytopathogenic Fungus *Sclerotinia sclerotiorum* Reveals Insights into the Genome Architecture of Broad Host Range Pathogens, *Genome Biology and Evolution*, Volume 9, Issue 3, March 2017, Pages 593–618, <https://doi.org/10.1093/gbe/evx030>
  24. Kariyawasam, G. K., Nelson, A. C., Williams, S. J., Solomon, P. S., Faris, J. D., & Friesen, T. L. (2023). The Necrotrophic Pathogen *Parastagonospora nodorum* Is a

Master Manipulator of Wheat Defense. *Molecular plant-microbe interactions* : *MPMI*, 36(12), 764–773. <https://doi.org/10.1094/MPMI-05-23-0067-IRW>

25. Grigoriev IV, Nordberg H, Shabalov I, Aerts A, Cantor M, Goodstein D, Kuo A, Minovitsky S, Nikitin R, Ohm RA, Otillar R, Poliakov A, Ratnere I, Riley R, Smirnova T, Rokhsar D, Dubchak I. *The Genome Portal of the Department of Energy Joint Genome Institute*. **Nucleic Acids Res.** 2012 Jan;40(Database issue):D26-32. <https://mycocosm.jgi.doe.gov/Aspac1/Aspac1.home.html>
26. Swilaiman, S. S., O'Gorman, C. M., Balajee, S. A., & Dyer, P. S. (2013). Discovery of a sexual cycle in *Aspergillus lentulus*, a close relative of *A. fumigatus*. *Eukaryotic cell*, 12(7), 962–969. <https://doi.org/10.1128/EC.00040-13>
27. Cao, Y., Cai, Q., Li, C., Song, G., Lu, N., & Yang, Z. (2023). Genome Sequence Resource of *Curvularia clavata* Causing Leaf Spot Disease on Tobacco by Oxford Nanopore PromethION. *Plant disease*, 107(6), 1916–1919. <https://doi.org/10.1094/PDIS-09-22-2283-A>
28. Grigoriev IV, Nordberg H, Shabalov I, Aerts A, Cantor M, Goodstein D, Kuo A, Minovitsky S, Nikitin R, Ohm RA, Otillar R, Poliakov A, Ratnere I, Riley R, Smirnova T, Rokhsar D, Dubchak I. *The Genome Portal of the Department of Energy Joint Genome Institute* **Nucleic Acids Res.** 2012 Jan;40(Database issue):D26-32. (N.d.). Retrieved from <https://mycocosm.jgi.doe.gov/Neudi1/Neudi1.home.html>
29. A.P. Douglas, S.C.-A. Chen, M.A. Slavin. Emerging infections caused by non-*Aspergillus* filamentous fungi. *Clinical Microbiology and Infection*, Volume 22, Issue 8. (2016)
30. Wenqiang Xia, Xiaoping Yu, Zihong Ye, Smut fungal strategies for the successful infection, *Microbial Pathogenesis*, Volume 142, 2020, 104039, ISSN 0882-4010, <https://doi.org/10.1016/j.micpath.2020.104039>. (<https://www.sciencedirect.com/science/article/pii/S0882401019310812>)
31. Fiorella Masotti, Betiana S Garavaglia, Natalia Gottig, Jorgelina Ottado, Bioremediation of the herbicide glyphosate in polluted soils by plant-associated microbes, *Current Opinion in Microbiology*, Volume 73, 2023, 102290, ISSN 1369-5274, <https://doi.org/10.1016/j.mib.2023.102290>. (<https://www.sciencedirect.com/science/article/pii/S1369527423000279>)
32. Sukno, SA García VM, Shaw BD, Thon MR 2008. Root Infection and Systemic Colonization of Maize by *Colletotrichum graminicola*. *Appl Environ Microbiol* 74: <https://doi.org/10.1128/AEM.01165-07>
33. *The Genome Portal of the Department of Energy Joint Genome Institute*, <https://mycocosm.jgi.doe.gov/Aspcam1/Aspcam1.home.html>  
Grigoriev IV, Nordberg H, Shabalov I, Aerts A, Cantor M, Goodstein D, Kuo A, Minovitsky S, Nikitin R, Ohm RA, Otillar R, Poliakov A, Ratnere I, Riley R, Smirnova T, Rokhsar D, Dubchak I. **Nucleic Acids Res.** 2012 Jan;40(Database issue):D26-32.
34. <https://mycocosm.jgi.doe.gov/Aspste1/Aspste1.home.html>, *The Genome Portal of the Department of Energy Joint Genome Institute*  
Grigoriev IV, Nordberg H, Shabalov I, Aerts A, Cantor M, Goodstein D, Kuo A, Minovitsky S, Nikitin R, Ohm RA, Otillar R, Poliakov A, Ratnere I, Riley R, Smirnova T, Rokhsar D, Dubchak I. **Nucleic Acids Res.** 2012 Jan;40(Database issue):D26-32.
35. Ben Hur P. Mobo, Peter M. Rabinowitz, Lisa A. Conti, Oyebo A. Taiwo, 12 - Occupational Health of Animal Workers, Editor(s): Peter M. Rabinowitz, Lisa A. Conti, Human-Animal



- Medicine, W.B. Saunders, (2010). <https://doi.org/10.1016/B978-1-4160-6837-2.00012-9>. Retrieved from <https://www.sciencedirect.com/science/article/pii/B9781416068372000129>
36. Urbina, J., Chestnut, T., Allen, J.M. *et al.* *Pseudogymnoascus destructans* growth in wood, soil and guano substrates. *Sci Rep* **11**, 763 (2021). <https://doi.org/10.1038/s41598-020-80707-1>
  37. <https://mycocosm.jgi.doe.gov/Magpo1/Magpo1.home.html>, The Genome Portal of the Department of Energy Joint Genome Institute  
Grigoriev IV, Nordberg H, Shabalov I, Aerts A, Cantor M, Goodstein D, Kuo A, Minovitsky S, Nikitin R, Ohm RA, Otiilar R, Poliakov A, Ratnere I, Riley R, Smirnova T, Rokhsar D, Dubchak I. **Nucleic Acids Res.** 2012 Jan;40(Database issue):D26-32.
  38. Yang, G., Jiang, L., Li, W., Li, E., & Lv, G. (2023). Structural Characteristics and Assembly Mechanisms of Soil Microbial Communities under Water-Salt Gradients in Arid Regions. *Microorganisms*, *11*(4), 1060. <https://doi.org/10.3390/microorganisms11041060>
  39. Pan, Y., She, D., Shi, Z., Cao, T., Xia, Y., & Shan, J. (2023). Salinity and high pH reduce denitrification rates by inhibiting denitrifying gene abundance in a saline-alkali soil. *Scientific reports*, *13*(1), 2155. <https://doi.org/10.1038/s41598-023-29311-7>
  40. Mundra, S., Kjønnaas, O. J., Morgado, L. N., Krabberød, A. K., Ransedokken, Y., & Kauserud, H. (2021). Soil depth matters: shift in composition and inter-kingdom co-occurrence patterns of microorganisms in forest soils. *FEMS microbiology ecology*, *97*(3), fiab022. <https://doi.org/10.1093/femsec/fiab022>
  41. US Department of Commerce, N. (2021). NWS Pueblo - Station Digest. Retrieved from <https://www.weather.gov/pub/stationDigest#:~:text=In%20general%2C%20Pueblo%20has%20a,days%20with%20sunshine%20each%20year>.
  42. S. Imada, K. Acharya, N. Yamanaka. Short-term and diurnal patterns of salt secretion by *Tamarix ramosissima* and their relationships with climatic factors. *Journal of Arid Environments*, Volume 83. 2012. <https://doi.org/10.1016/j.jaridenv.2012.03.006>.
  43. Fountain Creek Watershed District. 2025. <https://www.fountain-crk.org/fountain-creek-watershed>. Retrieved April 22<sup>nd</sup>, 2025.
  44. Theo Stein. Springs Utilities hit with Work Order, Fine. *Denver Post*, 2005. <https://www.denverpost.com/2005/10/06/springs-utilities-hit-with-work-order-fine/>
  45. Flood and Stormwater Management Attachment 1. Fountain Creek Watershed District. 2009. [https://www.fountain-crk.org/files/69459bd6f/App\\_C\\_Additional\\_Information\\_FloodingStormwater\\_Mgmt.pdf](https://www.fountain-crk.org/files/69459bd6f/App_C_Additional_Information_FloodingStormwater_Mgmt.pdf)
  46. Fountain Creek Watershed District. 2025. Overview. <https://www.fountain-crk.org/overview> Retrieved April 22<sup>nd</sup>, 2025.
  47. Love MI, Huber W, Anders S (2014). “Moderated estimation of fold change and dispersion for RNA-seq data with DESeq2.” *Genome Biology*, **15**, 550. [doi:10.1186/s13059-014-0550-8](https://doi.org/10.1186/s13059-014-0550-8).
  48. Basenko, E. Y., Pulman, J. A., Shanmugasundram, A., Harb, O. S., Crouch, K., Starns, D., Warrenfeltz, S., Aurrecoechea, C., Stoeckert, C. J., Jr, Kissinger, J. C., Roos, D. S., & Hertz-Fowler, C. (2018). FungiDB: An Integrated Bioinformatic Resource for Fungi and Oomycetes. *Journal of fungi (Basel, Switzerland)*, *4*(1), 39. <https://doi.org/10.3390/jof4010039>
  49. Quast C, Pruesse E, Yilmaz P, Gerken J, Schweer T, Yarza P, Peplies J, Glöckner FO (2013) The SILVA ribosomal RNA gene database project: improved data processing and web-based tools. *Nucl. Acids Res.* *41* (D1): D590-D596.

50. Yilmaz P, Parfrey LW, Yarza P, Gerken J, Pruesse E, Quast C, Schweer T, Peplies J, Ludwig W, Glöckner FO (2014) The SILVA and "All-species Living Tree Project (LTP)" taxonomic frameworks. [Nucl. Acids Res. 42:D643-D648](#)
51. Glöckner FO, Yilmaz P, Quast C, Gerken J, Beccati A, Ciuprina A, Bruns G, Yarza P, Peplies J, Westram R, Ludwig W (2017) 25 years of serving the community with ribosomal RNA gene reference databases and tools. [J. Biotechnol.](#)
52. Pruesse, E, Peplies, J and Glöckner, FO (2012) SINA: accurate high-throughput multiple sequence alignment of ribosomal RNA genes. [Bioinformatics, 28, 1823-1829](#)
53. McMurdie, P. J., & Holmes, S. (2013). Phyloseq: An R Package for Reproducible Interactive Analysis and Graphics of Microbiome Census Data. *PLOS ONE*, 8(4), e61217. <https://doi.org/10.1371/journal.pone.0061217>
54. Altschul SF, Gish W, Miller W, Myers EW, Lipman DJ (1990) "Basic local alignment search tool.". *J Mol Biol* 215: 403–410.
55. Schoch CL, et al. NCBI Taxonomy: a comprehensive update on curation, resources and tools. Database (Oxford). 2020: baaa062. [[PubMed](#)]
56. Sayers EW, et al. GenBank. Nucleic Acids Res. 2019. 47(D1):D94-D99. [[PubMed](#)]
57. Jake R Conway, Alexander Lex, Nils Gehlenborg, UpSetR: an R package for the visualization of intersecting sets and their properties, *Bioinformatics*, Volume 33, Issue 18, September 2017, Pages 2938–2940, <https://doi.org/10.1093/bioinformatics/btx364>